

Silk fibroin as an organic polymer for controlled drug delivery

Citation for published version (APA):

Hofmann, S., Foo, S., Rossetti, F., Textor, M., Vunjak-Novakovic, G., Kaplan, D. L., Merkle, H. P., & Meinel, L. (2006). Silk fibroin as an organic polymer for controlled drug delivery. *Journal of Controlled Release*, 111(1-2), 219-227. <https://doi.org/10.1016/j.jconrel.2005.12.009>

DOI:

[10.1016/j.jconrel.2005.12.009](https://doi.org/10.1016/j.jconrel.2005.12.009)

Document status and date:

Published: 01/01/2006

Document Version:

Accepted manuscript including changes made at the peer-review stage

Please check the document version of this publication:

- A submitted manuscript is the version of the article upon submission and before peer-review. There can be important differences between the submitted version and the official published version of record. People interested in the research are advised to contact the author for the final version of the publication, or visit the DOI to the publisher's website.
- The final author version and the galley proof are versions of the publication after peer review.
- The final published version features the final layout of the paper including the volume, issue and page numbers.

[Link to publication](#)

General rights

Copyright and moral rights for the publications made accessible in the public portal are retained by the authors and/or other copyright owners and it is a condition of accessing publications that users recognise and abide by the legal requirements associated with these rights.

- Users may download and print one copy of any publication from the public portal for the purpose of private study or research.
- You may not further distribute the material or use it for any profit-making activity or commercial gain
- You may freely distribute the URL identifying the publication in the public portal.

If the publication is distributed under the terms of Article 25fa of the Dutch Copyright Act, indicated by the "Taverne" license above, please follow below link for the End User Agreement:

www.tue.nl/taverne

Take down policy

If you believe that this document breaches copyright please contact us at:

openaccess@tue.nl

providing details and we will investigate your claim.

Silk fibroin as an organic polymer for controlled drug delivery

S. Hofmann^a, C.T. Wong Po Foo^b, F. Rossetti^c, M. Textor^c, G. Vunjak-Novakovic^d,
D.L. Kaplan^b, H.P. Merkle^a, L. Meinel^{a,b,e,*}

^a Drug Formulation and Delivery, ETH Zurich, 8093 Zurich, Switzerland

^b Department of Biomedical Engineering, Tufts University, Medford, MA 02155, USA

^c Surface Science and Technology, ETH Zurich, 8093 Zurich, Switzerland

^d Department for Bioengineering, Columbia University, New York, NY 10027, USA

^e Division of Health Sciences and Technology, M.I.T, Cambridge, MA 02139, USA

Received 17 August 2005; accepted 19 December 2005

Available online 3 February 2006

Abstract

The pharmaceutical utility of silk fibroin (SF) materials for drug delivery was investigated. SF films were prepared from aqueous solutions of the fibroin protein polymer and crystallinity was induced and controlled by methanol treatment. Dextrans of different molecular weights, as well as proteins, were physically entrapped into the drug delivery device during processing into films. Drug release kinetics were evaluated as a function of dextran molecular weight, and film crystallinity. Treatment with methanol resulted in an increase in β -sheet structure, an increase in crystallinity and an increase in film surface hydrophobicity determined by FTIR, X-ray and contact angle techniques, respectively. The increase in crystallinity resulted in the sustained release of dextrans of molecular weights ranging from 4 to 40 kDa, whereas for less crystalline films sustained release was confined to the 40 kDa dextran. Protein release from the films was studied with horseradish peroxidase (HRP) and lysozyme (Lys) as model compounds. Enzyme release from the less crystalline films resulted in a biphasic release pattern, characterized by an initial release within the first 36 h, followed by a lag phase and continuous release between days 3 and 11. No initial burst was observed for films with higher crystallinity and subsequent release patterns followed linear kinetics for HRP, or no substantial release for Lys. In conclusion, SF is an interesting polymer for drug delivery of polysaccharides and bioactive proteins due to the controllable level of crystallinity and the ability to process the biomaterial in biocompatible fashion under ambient conditions to avoid damage to labile compounds to be delivered.

© 2005 Elsevier B.V. All rights reserved.

Keywords: Drug delivery; Silk fibroin; FTIR; Wide angle X-ray scattering; Biomaterials

1. Introduction

Silks belong to a group of high molecular weight organic polymers characterized by repetitive hydrophobic and hydrophilic peptide sequences [1]. Due to the highly repetitive primary domains, fibrous proteins and especially silk fibroin (SF) assemble into regular structures during materials formation and can be considered as Nature's equivalents to synthetic block copolymers [1–5]. Silks are naturally produced by spiders or insects, such as *Nephila clavipes* and *Bombyx mori*, respectively [6,7]. The primary sequence of SFs have achieved wide evolutionary

adaptation to such diverse needs as spinning underwater nets to trap air for underwater breathing, lifelines, and prey capture, common features associated with the formation of robust and stable material structures. The repetitive organization and the presence of high contents of short side chain amino acids, glycine, serine, and alanine have been preserved in these protein polymer systems [8].

During the spinning process, several motifs in the silk form crystalline β -sheet stacks by hydrogen bonding and hydrophobic interactions, forming the basis for the tensile strength and toughness of the material [8–11]. This assembly process starts from highly concentrated silk solutions either in vivo or emulated in vitro. The protein assembly process in vivo is initiated by extraction of water, changes in salt concentration and finally triggered by mechanical stress or chain alignment during fiber

* Corresponding author. ETH Zurich, Department for Chemistry and Applied Biosciences, Room HCI J 390.1, Wolfgang-Pauli-Strasse 10, CH-8093 Zurich, Switzerland. Tel.: +41 44 633 73 85; fax: +41 44 633 13 14.

spinning. This process has been biomimetically transferred into *in vitro* environments, providing the basis for the fabrication of silk scaffolds as implant materials [12]. These silk-based biomaterials have interesting mechanical, morphological and structural properties that may fill important niches in biomaterial applications, in particular for the musculoskeletal system due to the robust mechanical properties [13–16].

The present study relates to the understanding of silk fibroin processing and control of structure development (β -sheet content as a reflection of degree of crystallinity) towards utility as a controlled release delivery matrix. The effect of the molecular weight of the compound to be delivered on the release kinetics from SF matrices was investigated within the context of control of crystalline content during processing. Furthermore, model proteins (enzymes) were formulated into the SF polymer films and their release pattern was followed with potency tests in order to extend the potential utility of this new controlled release device with bioactive molecules. The ability to formulate and control structural features of this family of proteins in an aqueous process suggests that sensitive biologicals can be incorporated into these matrices without significant loss of biological activity.

2. Materials and methods

2.1. Materials

Fluorescein isothiocyanate-dextrans with molecular weights of 4, 10, 20 and 40 kDa, respectively, horseradish peroxidase (HRP; EC 1.11.1.7.), lysozyme (Lys; EC 3.2.1.17), 2,2'-azino-bis(3-ethylbenzothiazoline-6-sulfonic acid) diammonium salt (ABTS), bovine serum albumin (BSA), *Micrococcus luteus*, 0.01 M phosphate-buffered saline (PBS: 2.7 mM potassium chloride, 0.137 M sodium chloride, pH 7.4) and *o*-phenylenediamine Fast Kit (OPD-Fast Kit; 0.4 mg/ml in 0.05 M phosphate-citrate buffer containing 0.4 mg/ml urea hydrogen peroxide) were from Sigma-Aldrich (Buchs, Switzerland), H₂O₂ was from Haenseler (Herisau, Switzerland). Purified polyclonal rabbit anti-chicken lysozyme antibody (80 mg/ml) and purified goat anti-rabbit IgG horseradish-peroxidase-linked antibody (2.0 mg/ml) were obtained from Acris Antibodies GmbH (Hiddenhausen, Germany). Silk was kindly supplied by Trudel Silk Inc. (Zurich, Switzerland). All other substances were of analytical or pharmaceutical grade and obtained from Sigma-Aldrich.

2.2. Film preparation

Cocoons from *B. mori* (Linne, 1758) were boiled 2 times for 1 h in an aqueous solution of 0.02 M Na₂CO₃ and rinsed with water as previously described [17]. Purified silk was solubilized in 9 M aqueous LiBr solution and dialyzed (Pierce, Woburn, MA; MWCO 3500 g/mol) against water for 2.5 days. Fibroin concentration was determined after evaporation of water overnight and using an analytical balance (Mettler, Greifensee, Switzerland). The concentration was adjusted to 5% (w/v). One hundred and fifty microliters of the silk fibroin solution was

transferred into polystyrene 96-well plates (for release study; Nunc, Wohlen, Switzerland) or onto flat Teflon surfaces (for physical characterization) and dried at 37 °C and 500 mbar overnight. Dried films were treated with 300 μ l of (i) 90% (v/v) methanol in H₂O or (ii) H₂O for 30 min, respectively or (iii), left untreated.

2.3. Film characterization

2.3.1. Atomic force microscopy (AFM)

Surface analysis of silk fibroin films, 6 mg each and either treated with 90% methanol (v/v) or left untreated, was performed in contact mode using a Nanoscope IIIa (Digital Instruments, San Diego, CA) with oxide-sharpened Si₃N₄ tips mounted on triangular cantilevers with spring constants of 0.58 N/m (specified by the manufacturer). Images were taken in air and flattened and plane-fitted as required.

2.3.2. Fourier-transform infrared spectroscopy (FTIR)

Compound-loaded and unloaded (empty) films were prepared and either methanol treated or left untreated as described before. The structure of the various films was analyzed by FTIR on a Bruker Equinox 55 Spectrometer equipped with a MIRacle™ attenuated total reflection (ATR) Ge crystalline cell in reflection mode. Background measurements were taken twice with an empty cell and subtracted from the sample readings.

2.3.3. Wide angle X-ray scattering (WAXS)

Real-time wide angle X-ray scattering studies were performed at beamline X27C of the National Synchrotron Light Source (NSLS; Brookhaven National Laboratory, NY). Intensity data were collected at room temperature with films encapsulated in Kapton™ tape. Monochromatic X-radiation with a wavelength of $\lambda=0.15$ nm was used. The data were collected in transmission mode using two one-dimensional position sensitive wire detectors. The scattering vectors, q ($q=4\pi \cdot \sin\theta / \lambda$, with θ as the half-scattering angle) were calibrated using sodalite and silicon reference powders for WAXS. Scans were collected for 3 min over an angular range from $2\theta=10$ – 30° . Intensity data were corrected to account for detector linearity, background scattering, sample absorption, and changes in incident beam intensity. Due to the detector geometry, the range of angles from $2\theta=1$ – 7° was not accessible at NSLS. Therefore, room temperature WAXS studies were performed using a conventional sealed tube X-ray source having $\lambda=0.15$ nm. A Phillips PW1830 X-ray generator and optically encoded diffractometer were used to investigate the range of scattering angles at which the OMS typically shows its gallery spacing, i.e. from $2\theta=2$ – 7° . Films were examined in $\theta/2\theta$ reflection mode, using a step scan interval of 0.01° with 2.4 s/step; d -spacings, obtained from Bragg's Law ($n\lambda=2d \cdot \sin\theta$; where λ is the wavelength of the beam of X-rays and is equal to 0.15 nm, θ is the angle of incidence in degrees, and d is the spacing between atomic planes and is given here in nm).

2.3.4. Contact angle

Static contact angle measurements were performed on dry films ($n=3$) that were either treated with 90% (v/v) methanol or

untreated at ambient temperature using a goniometer (NRL C, Ramé-hart Inc., Mountain Lakes, NJ). Ultrapure water droplets were used with a drop volume of approximately 30 μl .

2.4. Drug load and release

The silk fibroin solution (5% *w/v*) was mixed with a drug solution in either PBS (10 mg/ml; FITC-dextran) or PBS+0.1% (*m/v*) BSA (10 mg/ml; HRP, Lys) at a ratio of 7.5:1 (*v/v*), respectively. One-hundred and fifty microliters per well of this mixture or 150 μl silk fibroin solution (5% *w/v*) was pipetted into polystyrene 96-well plates. Films were dried overnight (37 °C; 500 mbar) and treated with methanol or water as described above. The supernatant was collected and the solvent was evaporated using a speedvac concentrator (sc110, Savant, Fisher Scientific, Wohlen, Switzerland). Residues were redissolved in 300 μl PBS (FITC-dextran) or PBS+0.1% (*m/v*) BSA (HRP, Lys) and the compound content in the supernatant was measured as described later. The films were dried again at 37 °C and 500 mbar overnight. For release studies, 300 μl of release medium was added to each well and the plates were incubated at 25 °C for 23–28 days. At each time point the whole medium was collected for measurement and replaced by fresh release medium (Table 1).

2.4.1. Size exclusion chromatography (SEC) of FITC-dextran

FITC-dextran were assayed by SEC-chromatography using a Merck system (Dübelndorf, Switzerland), consisting of an auto-sampler (Merck Hitachi AS), a computer interface (Merck Hitachi A6000), a pump (Merck Hitachi L6200A) and a fluorescence detector (Merck Hitachi F-1050). Separation was performed on a Superdex® 200 HR 10/30 column (Amersham Biosciences Europe, Otelfingen, Switzerland) at 4 °C with 50 nM phosphate buffer (pH 7.4) at a flow rate of 0.5 ml/min. FITC-dextran fluorescence was detected with an excitation wavelength of 485 nm and an emission wavelength of 530 nm.

2.4.2. HRP activity assay

The enzyme solutions were diluted in a solution which consisted of 0.5% (*v/v*) Triton-X 100 and 0.25% (*w/v*) BSA in 40 mM potassium phosphate buffer at pH 6.8. Ten microliter

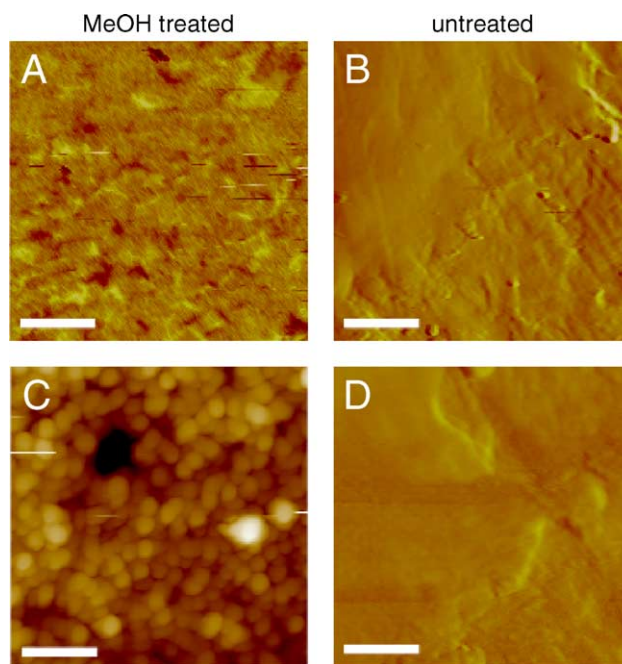


Fig. 1. AFM images of silk film surfaces either treated with 90% methanol (A, C) or left untreated (B, D). (A, B): bar length 2.5 μm , (C, D): bar length 0.5 μm .

samples or standards were added to 200 μl freshly prepared substrate solution (0.5 mg/ml ABTS and 0.03% (*w/v*) H_2O_2 in 100 mM citrate buffer at pH 4.1) and the absorption was read at 405 nm at 25 °C using a spectrophotometer (Cary 300; Palo Alto, CA).

2.4.3. Lys activity assay

Lys activity was determined by turbidity measurements with *M. luteus* cell suspension in 50 mM potassium phosphate buffer at pH 7. The cells were mortared and suspended in 50 mM potassium phosphate buffer until the absorption was in the range of 0.7–0.9 as measured at 450 nm. Twenty-five microliter lysozyme solution was added to 1.5 ml cell suspension and the decrease in absorption (450 nm) was read for 5 min. The maximum linear rates for samples, standards and blank were obtained and the activity of the enzyme was calculated.

2.4.4. ELISA for lys quantification

For quantification of released Lys protein, an indirect ELISA procedure modified from Vidal et al. [18] was performed. Incubation was at room temperature (25 °C) on a rotating microplate shaker (IKA Labortechnik, Staufen, Germany). Flat-bottom 96-well polystyrene microtiter plates (Nalge Nunc, Hereford, UK) were washed with PBS between every step of the assay and 4 times at each step (100 μl /well except after blocking: 200 μl /well). Reactant volumes were 50 μl /well. Microplates were initially coated for 2 h with Lys in PBS and nonspecific sites were blocked for 1 h using a solution of 3% BSA (*w/v*) in PBS. Polyclonal rabbit anti-chicken lysozyme antibody and goat anti-rabbit IgG horseradish peroxidase-linked antibody in 1% BSA-TPBS (1% (*w/v*) BSA-PBS plus 0.05% (*w/v*) Tween 20) were subsequently added and incubated for 2 h. The substrate (OPD

Table 1
Physicochemical properties of model drugs

Compound	Molecular weight [kDa]	Release medium	Radius [nm]	<i>pI</i>
FD4	4	PBS	1.4 ^a	–
FD10	10	PBS	2.3 ^a	–
FD20	20	PBS	3.3 ^a	–
FD40	40	PBS	4.5 ^a	–
HRP type VI-A	44	PBS+0.1% BSA	3 ^b	6–9 ^c
Lys	14.3	PBS+0.1% BSA	1.8 ^b	11.35

^a Approximate Stoke's radii given by the supplier.

^b Solute radius was calculated from aqueous diffusivities found in the literature using the Stokes–Einstein equation.

^c Depending on the isoenzyme.

at 0.4 mg/ml in 0.05 M phosphate–citrate buffer containing 0.4 mg/ml urea hydrogen peroxide) for peroxidase was placed in the wells for 15 min. The reaction was stopped by the addition of 50 μ l 1 M H₂SO₄. Absorbance was read at 540 nm using a microplate reader (Molecular Devices, Bucher Biotec AG, Basel, Switzerland).

2.4.5. Gel filtration chromatography (GFC) for lysozyme

Lys was assayed for aggregation and degradation products by GFC-chromatography using a Merck system (Duebendorf, Switzerland), consisting of an autosampler (Merck Hitachi AS), a computer interface (Merck Hitachi A6000), a pump (Merck Hitachi L6200A) and a UV/VIS detector (Merck Hitachi L-4250). Separation was performed on a Shodex protein KW804 column (Infochroma AG, Zug, Switzerland) at 25 °C with 50 mM

phosphate buffer with 0.3 M sodium chloride (pH 7.5) at a flow rate of 1.0 ml/min. Lys absorption was detected at 274 nm.

2.4.6. Protein adsorption to silk films

Three hundred microliter protein solution (HRP: 1 mg/ml; Lys: 10 mg/ml) in PBS containing 0.1% BSA was added to either methanol treated or non-methanol treated films and incubated at 25 °C for 24 h. Adsorption of the proteins to the silk films was determined by measuring the reduction of protein activity in the supernatant.

2.5. Statistical analysis

For statistical significance, samples were evaluated using a Student *t*-test as well as ANOVA where appropriate. ANOVA

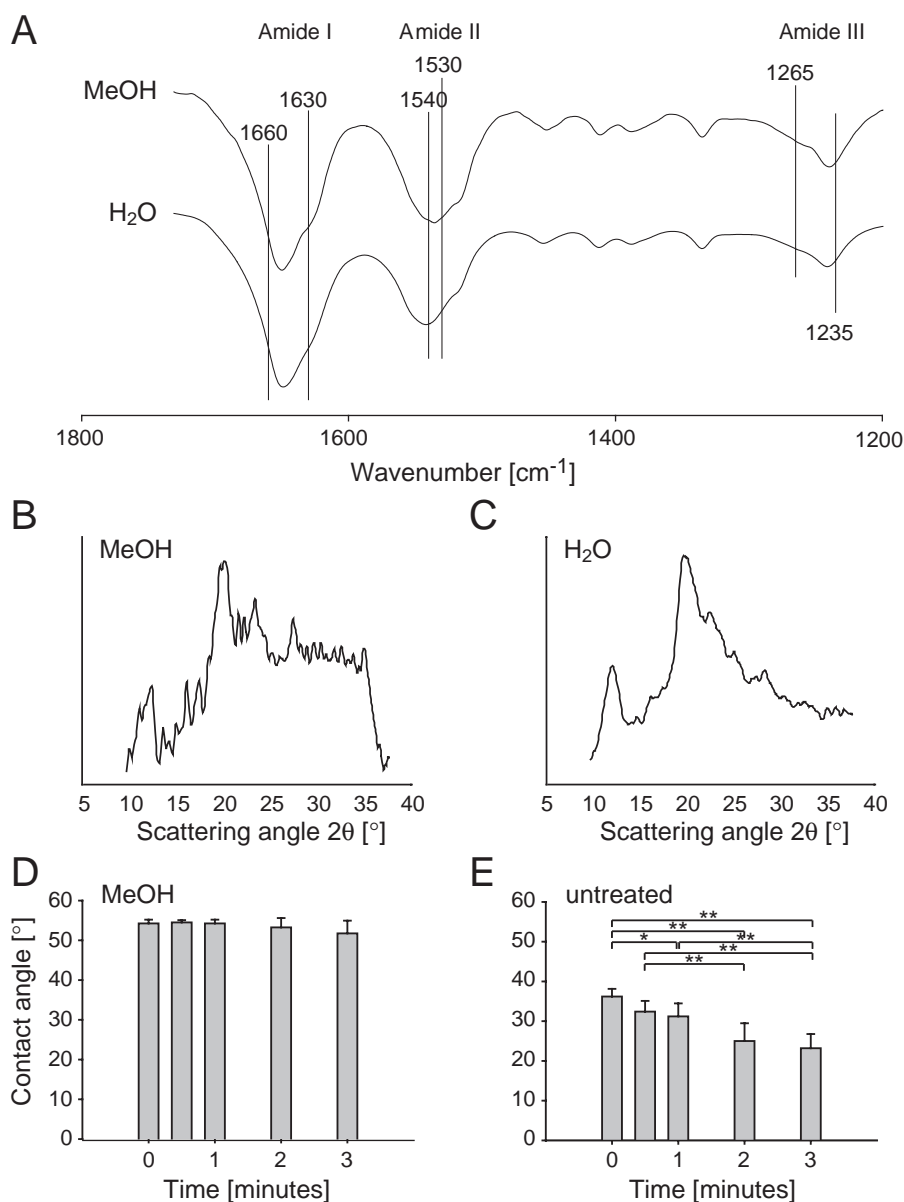


Fig. 2. Physicochemical characterization of silk films either untreated or treated with water or 90% methanol. (A) FTIR spectra of methanol or water treated silk films; determination of crystallinity by XRD of methanol treated (B) and water treated (C) films; determination of hydrophilicity/hydrophobicity of the film surface by contact angle measurements of methanol treated (D) and non-methanol treated (E) films over time.

was followed by a post-hoc assessment using the Tukey HSD method. Differences were considered significant when equal or less than $p=0.05$.

3. Results

3.1. Surface characterization and physicochemical analysis of silk films

Silk film morphology was assessed by atomic force microscopy before and after methanol treatment (Fig. 1). Methanol treatment resulted in rougher surfaces when compared to non-methanol treated films and the formation of globular structures, which were not found in native (i.e. not methanol treated) films. FTIR structural analysis of methanol treated films showed an N–H bending vibration bond (amide II) intensity shift from 1540 to 1535 cm^{-1} when compared to native films (Fig. 2A). Similarly, methanol treatment resulted in additional shoulders at 1630 cm^{-1} (amide I) and 1265 cm^{-1} (amide III). The water treated silk films for the most part lack the peaks for secondary structure at 1695 , 1627 and 1520 cm^{-1} , however, it seems as though with the

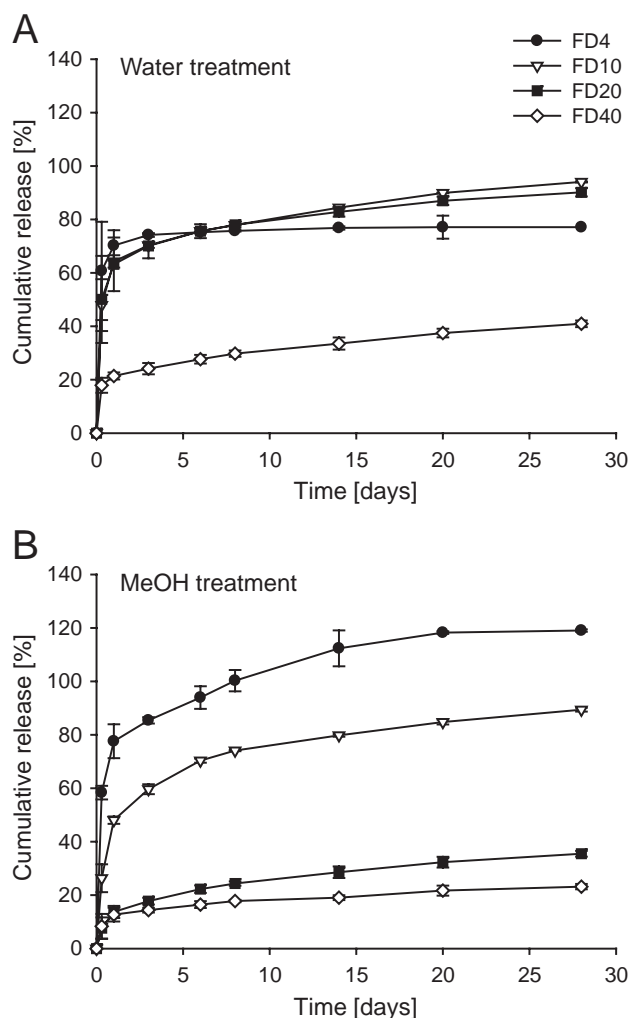


Fig. 3. Cumulative release of different molecular masses of FITC-dextrans from silk fibroin films treated with H₂O (A) or 90% methanol (B). ●—FD4, ▽—FD10, ■—FD20, ◇—FD40.

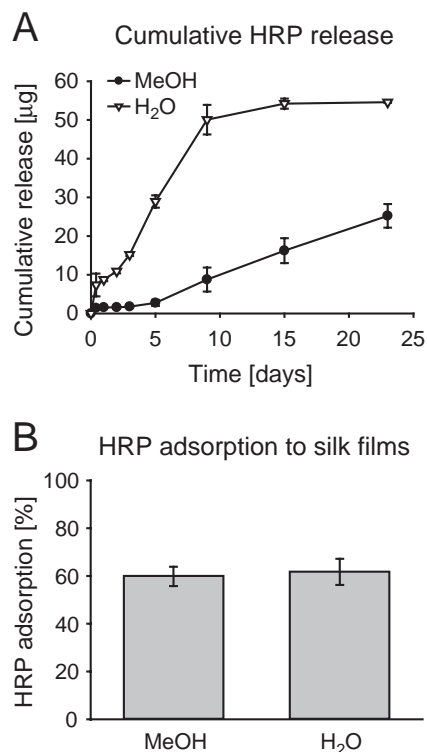


Fig. 4. Interaction of horseradish peroxidase with silk films: (A) Cumulative release of HRP from silk films treated with either 90% methanol or H₂O, respectively. (B) Adsorption of HRP from an aqueous solution to a silk fibroin surface either treated with 90% methanol or non-methanol treated.

addition of FD20 and FD40, the FTIR structures start showing a more pronounced shoulder or peak at ~ 1627 and 1515 cm^{-1} indicating an increase in β -sheet conformation for those films. These data were corroborated by wide-angle X-ray scattering (WAXS) also used in the material characterization (Fig. 2B, C). With WAXS, silk crystallinity was monitored by calculating the intersheet d -spacing distances from the X-ray plots. Methanol treatment resulted in a shift of the major peak ($2\theta=20^\circ$; Fig. 2B, C) from 4.4 to 4.3 \AA , indicating a shift from silk I to silk II structure. For comparison with our data, representative silk I and silk II model structures that had been taken by X-ray and electron diffraction, infrared spectroscopy, nuclear magnetic resonance, and raman spectroscopy were collected from literature [19–30] and resulted in three predictions of silk I structure models, the Crankshaft model [26], the out-of-register model [23] and the repeated β -turn type II model [20]. Silk II structure is commonly described by antiparallel β -sheets [31,32]. More peaks corresponding to reported silk II β -sheet crystalline structures were present in the methanol treated films including the shift in the position of the major peak at $2\theta=20^\circ$, indicating a shift from silk I to the more dense silk II structure (data not shown).

Film surface hydrophobicity of methanol treated silk films showed a significantly higher contact angle than for non-methanol treated films at each time-point ($p<0.001$; Fig. 2D, E). Contact angles remained stable for methanol treated films (Fig. 2D) whereas a significant drop over time was observed for non-methanol treated films ($p<0.05$ or $p<0.01$; Fig. 2E).

3.2. Compound release

The release of fluorescently labelled dextrans (FD) with molecular weights ranging from 4 (FD4) to 40 kDa (FD40), respectively, was evaluated as a function of methanol treatment using HPLC quantification (Fig. 3, Table 1). In water treated films, FDs with molecular weights from 4 to 20 kDa showed a burst release after 8 h of $60.7 \pm 30\%$, $47.9 \pm 20\%$ and $50 \pm 32\%$, respectively. Later than 3 days, FD4-release ceased almost completely ($77 \pm 6\%$ after 28 days), while FD10 and FD20 showed a continuous release pattern up to $94.0 \pm 0.2\%$ and $90.2 \pm 1.7\%$ after 28 days, respectively. In contrast, the release of the larger molecule FD40 was retarded and showed an initial release of only $17.9 \pm 15\%$ followed by a continuous release to up to $40.9 \pm 3\%$ after 28 days (Fig. 3A). Methanol treatment of the drug loaded silk films resulted in a strong and molecular weight dependent retardation of the release of all FDs. Burst releases of FD4, FD10, FD20 and FD40 were $58.4 \pm 4\%$, $26.3 \pm 19\%$, $7.7 \pm 52\%$ and $8.4 \pm 55\%$, respectively. With an increase in molecule size, a reduction of the incline

was observed for the first 10 days of release, levelling off after 14 days for all molecules (Fig. 3B).

Further studies detailed the efficacy of silk fibroin films as delivery vehicles for bioactive compounds, using HRP and Lys as model drugs (Figs. 4 and 5, Table 1), based on bioactivity assessments. A discontinuous release from non-methanol treated silk films was observed for HRP, characterized by an initial burst of $7.4 \pm 0.3 \mu\text{g}$, followed by a lag phase of 2 days and a continuous release from days 3 to 8. At later timepoints, no more release of bioactive HRP was measured (Fig. 4A). HRP release from methanol treated films started at day 5 and continued until day 23, with a total release of $25.2 \pm 3.0 \mu\text{g}$ HRP (Fig. 4A). The affinity of HRP to the silk films was measured upon incubation of non-methanol treated and methanol treated silk films with the model drug for 24 h. HRP demonstrated strong affinity to the silk fibroin surface, but no significant differences were observed for the two treatments (Fig. 4B).

Bioactive Lys release from non-methanol treated silk films was characterized by an initial burst of about $21.3 \pm 12.9 \mu\text{g}$, followed by a short lag phase and a continuous release between days 3

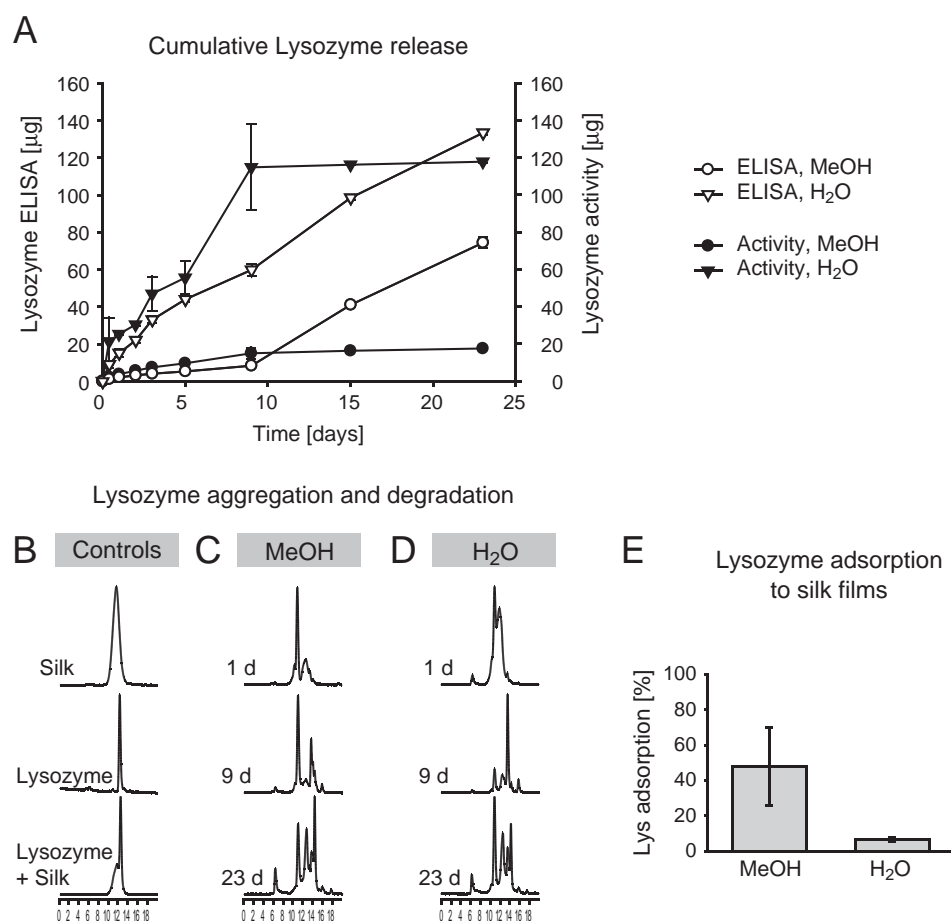


Fig. 5. Interaction of lysozyme with silk films: (A) Cumulative release of Lys from silk films treated with either 90% methanol or H₂O, respectively. Data are presented as amount of protein released as measured with ELISA (open symbols) or amount of protein released as calculated from the activity measurements (black symbols). (B, C, D) SE-HPLC measurements showing: silk, Lys and a mixture of both in release buffer as controls (B), released molecules out of silk films treated with 90% methanol (C) or water (D) after 1, 9 and 23 days, respectively. (E) Adsorption of Lys from an aqueous solution to a silk fibroin surface either treated with 90% methanol or non-methanol treated.

and 8 (Fig. 5A). After 9 days of release, no bioactive Lys was released. No bioactive Lys was detected from methanol treated films throughout the study time (Fig. 5A). However, ELISA measurements of the amount of released protein by ELISA using a polyclonal Lys antibody showed a release from methanol treated silk films, starting at day 8 with a continuous and linear release pattern thereafter and—although at a lower level—parallel to the release from non-methanol treated films (Fig. 5A). The released Lys was further analyzed to detail the cause of the positive ELISA and negative potency results, using qualitative GFC-HPLC studies. Clearly, by-products of lower size (degraded) and higher size (aggregates) of Lys were released in the incubation medium and their presence increased with time for both, methanol (Fig. 5C) and non-methanol treated (Fig. 5D) films. An apparent silk peak was observed at early timepoints and for the water treated—and better water soluble—silk films as compared to the methanol treated ones, and overlap was observed for the silk peak and the Lys peak (Fig. 5B, D). This observed degradation phenomenon correlates with measurements of weight loss of non-methanol treated silk films in PBS (data not shown). The adsorption of Lys was slightly higher for methanol treated as observed to non-methanol treated films, but not significant ($p=0.08$; Fig. 5E).

4. Discussion

Silk fibroin is isolated from cocoons of the silkworm, *B. mori*. This protein has recently found growing interest as a biomaterial for musculoskeletal implants, including substrates for tissue engineered cartilage, bone, and ligaments [14–16,33,34]. Several studies detail the advantages of SF based materials, including the directed differentiation of human mesenchymal stem cells (MSC) into different tissues and excellent biocompatibility [13,35,36]. Furthermore, the mechanical properties of SF in fiber form, rivaling high performance fibers such as Kevlar in terms of energy adsorbed before the fiber breaks, distinguish this organic polymer from other naturally occurring alternatives, such as collagen [37].

MSC differentiate selectively along different lineages including cartilage and bone, when exposed to specific proteins—e.g. growth factors and cytokines. Ideally, a scaffold material provides a substrate in which cells can thrive and receive stimuli such as through protein release to guide the differentiation process of cells. Therefore, this study evaluated SF as a delivery vehicle for the sustained release of compounds and enzymes as model drugs to further expand the material options available with SF in the important niche of controlled release. Earlier studies have demonstrated the use of silk fibroin carriers for enzyme immobilization as needed for the preparation of biosensors [38,39]. These studies detailed the protective properties of silk fibroin matrices for several proteins including staphylococcal protein A [40], alkaline phosphatase [38], and various other proteins and peptides [41,42]. Ultimately, this type of materials system could lead to a novel mechanically useful implant material, stabilizing and releasing proteins that guide the differentiation process of cells in a directed fashion through controlled drug delivery.

Methanol treatment of the silk films resulted in physicochemical changes with the formation of globular surface structures which were absent on surfaces from water treated films (Fig. 1). Further, methanol treatment induced a shift to higher amounts of crystalline β -sheets structures (Fig. 2A, B) and resulted in higher hydrophobicity as indicated by contact angle measurements (Fig. 2D, E). The different crystalline states were detected by FTIR spectra, resulting in a typical shift for amide III bond stretching (1235 and 1265 cm^{-1}) and changes in the amide V bond regions. In particular the shoulder in the amide III band region is indicative for a conformational shift of silk fibroin into β -sheet structure, as described before [31,43]. Changes in silk assembly as a result from a silk I to a silk II conformational change were further detailed by wide angle X-ray scattering (WAXS) before and after methanol treatment. The assembly of silk fibers in the silk I conformation state was described by three different models, obtained through measurements of d-spacing data from WAXS, the Crankshaft [44], β -turn type II [23] and the out of register [20,21,31] model, respectively. Assembly in silk structures with a silk II conformational state and as a result of methanol treatment was presented by Marsh et al. [32] and Asakura and colleagues [20,21,31]. A comparison of d-spacing from WAXS spectra and taken from water treated (mainly silk-I conformation) films in this study (extracted from Fig. 2B, C), fitted best with the out-of-register model of silk assembly, which was subject to substantial changes after methanol treatment, resulting in structures of a silk-II conformational state and as previously described [21,32].

For evaluation of drug size/molecular weight impact on release patterns, dextrans with increasing sizes and molecular weights were used. Dextrans with molecular weights of 2 to 10 kDa arrange in expandable coils, whereas dextrans with molecular weights exceeding 10 kDa organize in branched structures [45,46]. The higher the molecular weight, the larger was the retention of the drug, more specifically for methanol treated films (Fig. 3). These retentions were a result of the above described changes in physicochemical properties, characterized by an increase of crystalline β -sheets and a concomitant decrease in water solubility [12,47,48], ultimately resulting in more sustained release kinetics.

In the present study, crystallinity was induced by methanol treatment [1,5,12,49], which can be detrimental to the bioactivity of a drug, in particular for protein drugs [50]. These detrimental methanol effects were observed for lysozyme by comparative experiments of drug release into the supernatant using an ELISA and a potency assay (Fig. 5). Lys release from water treated films resulted in similar release profiles as measured by the two different assays (potency versus presence of antigen), whereas a substantial loss in bioactivity was determined for drugs released from methanol treated films. Therefore, silk scaffolds failed to protect lysozyme potency after methanol treatment. Interestingly, HRP entrapment into methanol treated films resulted in a release of bioactive HRP (Fig. 4), whereas complete loss of potency resulted from methanol supplementation to aqueous HRP solutions (data not shown). Based on these findings, a selective protection for protein drugs can be postulated for silk biopolymers. Future studies are needed detailing the mechanistic principles of protection by silks.

Drug release kinetics were further influenced by the drug's nature, as can be exemplarily seen with a comparison of HRP (Stoke's radius of approximately 3 nm) and FD20 (Stoke's radius of 3.3 nm). Apart from similarities in diameters, both HRP and FD20 resulted in completely different release patterns. Therefore, easy predictions of drug release kinetics from silks are difficult and call for a clear need to individually assess a drug's retention within the biopolymer.

The experiments highlight the strength but also the limitations of using silk fibroin as a polymer for drug delivery. The motivation of this study was to combine the excellent biomaterial properties of silks—biocompatibility, mechanical integrity, and biodegradation—with drug delivery options. We believe a general feasibility of this approach can be postulated from the presented work, although detrimental effects of processing steps involving the use of methanol on drug potency need to be addressed for each individual drug intended to be delivered. Further, adsorption to silk surfaces can significantly—and again as a result of individual drug properties—change drug release kinetics. Current experiments in our lab aim at using repetitive cycles of water vapor exposition instead of methanol treatment to induce changes in silk crystallinity, to by-pass the detrimental effects of methanol. Preliminary own results and supporting data from literature [51] suggest the feasibility of this replacement, while maintaining suitable drug delivery kinetics similar to the ones shown for methanol treated films.

An envisioned scenario for the above introduced system in tissue engineering would be the use of drug releasing SF biomaterials to guide the differentiation of MSC into musculo-skeletal tissues. A close monitoring of drug potency and aggregation phenomena is required to optimize such systems. These systems offer preservation of sensitive protein activity, allow for a controlled and sustained delivery of proteins, along with control of scaffold structure and morphology. When these features are considered along with the remarkable mechanical properties of these proteins in materials, intriguing options for new biomaterial utility for this family of proteins begin to emerge.

Acknowledgements

We thank Prof. Peggy Cebe and Xiao Hu for their help in XRD data acquisition at the XY synchrotron (Brookhaven, MD), and Trudel Inc. (Zurich Switzerland) for cocoon supply. Financial support from NIH (EB00252 and EB003210), the NSF (DMR) and the Association for Orthopedic Research (AFOR) is greatly appreciated.

References

- [1] R. Valluzzi, S. Winkler, D. Wilson, D.L. Kaplan, Silk: molecular organization and control of assembly, *Philos. Trans. R. Soc. Lond., B Biol. Sci.* 357 (1418) (2002) 165–167.
- [2] X. Chen, D.P. Knight, Z. Shao, F. Vollrath, Conformation transition in silk protein films monitored by time-resolved Fourier transform infrared spectroscopy: effect of potassium ions on *Nephila spidroin* films, *Biochemistry* 41 (50) (2002) 14944–14950.
- [3] J.D. van Beek, S. Hess, F. Vollrath, B.H. Meier, The molecular structure of spider dragline silk: folding and orientation of the protein backbone, *Proc. Natl. Acad. Sci. U. S. A.* 99 (16) (2002) 10266–10271.
- [4] F. Vollrath, B. Madsen, Z. Shao, The effect of spinning conditions on the mechanics of a spider's dragline silk, *Proc. R. Soc. Lond., B Biol. Sci.* 268 (1483) (2001) 2339–2346.
- [5] D. Wilson, R. Valluzzi, D. Kaplan, Conformational transitions in model silk peptides, *Biophys. J.* 78 (5) (2000) 2690–2701.
- [6] D.P. Knight, F. Vollrath, Biological liquid crystal elastomers, *Philos. Trans. R. Soc. Lond., B Biol. Sci.* 357 (1418) (2002) 155–163.
- [7] F. Vollrath, D.P. Knight, Liquid crystalline spinning of spider silk, *Nature* 410 (6828) (2001) 541–548.
- [8] G.H. Altman, F. Diaz, C. Jakuba, T. Calabro, R.L. Horan, J. Chen, H. Lu, J. Richmond, D.L. Kaplan, Silk-based biomaterials, *Biomaterials* 24 (3) (2003) 401–416.
- [9] G.H. Altman, H.H. Lu, R.L. Horan, T. Calabro, D. Ryder, D.L. Kaplan, P. Stark, I. Martin, J.C. Richmond, G. Vunjak-Novakovic, Advanced bioreactor with controlled application of multi-dimensional strain for tissue engineering, *J. Biomech. Eng.* 124 (6) (2002) 742–749.
- [10] K.H. Guhrs, K. Weissart, F. Grosse, Lessons from nature-protein fibers, *J. Biotechnol.* 74 (2) (2000) 121–134.
- [11] Z. Shao, F. Vollrath, Surprising strength of silkworm silk, *Nature* 418 (6899) (2002) 741.
- [12] H.J. Jin, D.L. Kaplan, Mechanism of silk processing in insects and spiders, *Nature* 424 (6952) (2003) 1057–1061.
- [13] L. Meinel, S. Hofmann, V. Karageorgiou, C. Kirker-Head, J. McCool, G. Gronowicz, L. Zichner, R. Langer, G. Vunjak-Novakovic, D.L. Kaplan, The inflammatory responses to silk films in vitro and in vivo, *Biomaterials* 26 (2) (2005) 147–155.
- [14] L. Meinel, S. Hofmann, V. Karageorgiou, L. Zichner, R. Langer, D. Kaplan, G. Vunjak-Novakovic, Engineering cartilage-like tissue using human mesenchymal stem cells and silk protein scaffolds, *Biotechnol. Bioeng.* 88 (3) (2004) 379–391.
- [15] L. Meinel, V. Karageorgiou, R. Fajardo, B. Snyder, V. Shinde-Patil, L. Zichner, D. Kaplan, R. Langer, G. Vunjak-Novakovic, Bone tissue engineering using human mesenchymal stem cells: effects of scaffold material and medium flow, *Ann. Biomed. Eng.* 32 (1) (2004) 112–122.
- [16] L. Meinel, V. Karageorgiou, S. Hofmann, R. Fajardo, B. Snyder, C. Li, L. Zichner, R. Langer, G. Vunjak-Novakovic, D.L. Kaplan, Engineering bone-like tissue in vitro using human bone marrow stem cells and silk scaffolds, *J. Biomed. Mater. Res.* 71A (1) (2004) 25.
- [17] S. Sofia, M.B. McCarthy, G. Gronowicz, D.L. Kaplan, Functionalized silk-based biomaterials for bone formation, *J. Biomed. Mater. Res.* 54 (1) (2001) 139–148.
- [18] M.L. Vidal, J. Gautron, Y. Nys, Development of an ELISA for quantifying lysozyme in hen egg white, *J. Agric. Food Chem.* 53 (7) (2005) 2379–2385.
- [19] J.P. Anderson, Morphology and crystal structure of a recombinant silk-like molecule, SLP4, *Biopolymers* 45 (1998) 307–321.
- [20] T. Asakura, J. Ashida, T. Yamane, T. Kameda, Y. Nakazawa, K. Ohgo, K. Komatsu, A repeated beta-turn structure in poly(Ala-Gly) as a model for silk I of *Bombyx mori* silk fibroin studied with two dimensional spin-diffusion NMR under off magic angle spinning and rotational echo double resistance, *J. Mol. Biol.* 306 (2) (2001) 291–305.
- [21] T. Asakura, M. Demura, T. Date, N. Miyashita, K. Ogawa, M.P. Williamson, NMR study of silk I structure of *Bombyx mori* silk fibroin with N-15- and C-13-NMR chemical shift contour plots, *Biopolymers* 41 (1997) 193–203.
- [22] T. Asakura, T. Yamane, Y. Nakazawa, T. Kameda, K. Ando, Structure of *Bombyx mori* silk fibroin before spinning in solid state studied with wide angle X-ray scattering and ¹³C cross-polarization/magic angle spinning NMR, *Biopolymers* 58 (5) (2001) 521–525.
- [23] S.A. Fossey, G. Nemethy, K.D. Gibson, H.A. Scheraga, Conformational energy studies of beta-sheets of model silk fibroin peptides: I. Sheets of poly(Ala-Gly) chains, *Biopolymers* 31 (13) (1991) 1529–1541.
- [24] S.J. He, R. Valluzzi, S.P. Gido, Silk I structure in *Bombyx mori* silk foams, *Int. J. Biol. Macromol.* 24 (1999) 187–195.
- [25] O. Kratky, E. Schauenstein, A. Sekora, An unstable lattice in silk fibroin, *Nature* 165 (1950) 319–320.

- [26] B. Lotz, H.D. Keith, Crystal structure of poly(L-Ala-Gly)II. A model for silk. I, *J. Mol. Biol.* 61 (1) (1971) 201–215.
- [27] P. Monti, P. Taddei, G. Freddi, T. Asakura, M. Tsukada, Raman spectroscopic characterization of *Bombyx mori* silk fibroin: raman spectrum of silk I, *J. Raman Spectrosc.* 32 (2001) 103–107.
- [28] K. Okuyama, R. Somashekar, K. Noguchi, S. Ichimura, Refined molecular and crystal structure of silk I based on Ala-Gly and (Ala-Gly)(2)-Ser-Gly peptide sequence, *Biopolymers* 59 (2001) 310–319.
- [29] H. Saito, Y. Iwanga, R. Tabeta, M. Narita, T. Asakura, High-resolution C-13 NMR-study of silk fibroin in the solid state by the cross-polarization magic angle spinning method—conformational characterization of silk-I and silk-II type forms of *Bombyx-mori* fibroin by the conformation-dependent C-13 chemical shifts, *Macromolecules* 17 (1984) 1405–1412.
- [30] T. Yamane, K. Umemura, Y. Nakazawa, T. Asakura, Molecular dynamics simulation of conformational change of poly(Ala-Gly) from silk I to silk II in relation to fiber formation mechanism of *Bombyx mori* silk fibroin, *Macromolecules* 36 (2003) 6766–6772.
- [31] T. Asakura, A. Kuzuhara, R. Tabeta, H. Saito, Conformation characterization of *Bombyx mori* silk fibroin in the solid-state by high-frequency C-13 cross-polarization magic angle spinning NMR, X-Ray Diffraction, and Infrared Spectroscopy, *Macromolecules* 18 (1985) 1841–1845.
- [32] R.E. Marsh, R.B. Corey, L. Pauling, An investigation of the structure of silk fibroin, *Biochim. Biophys. Acta* 16 (1) (1955) 1–34.
- [33] G.H. Altman, R.L. Horan, H.H. Lu, J. Moreau, I. Martin, J.C. Richmond, D.L. Kaplan, Silk matrix for tissue engineered anterior cruciate ligaments, *Biomaterials* 23 (20) (2002) 4131–4141.
- [34] L. Meinel, V. Karageorgiou, S. Hofmann, R. Fajardo, B. Snyder, C. Li, L. Zichner, R. Langer, G. Vunjak-Novakovic, D. Kaplan, Tissue engineering of osteochondral plugs using human mesenchymal stem cells and silk scaffolds, *Chem. Ind.* 58 (6a) (2004) 68–69.
- [35] B. Panilaitis, G.H. Altman, J. Chen, J. Hyoun-Joon, V. Karageorgiou, D.L. Kaplan, Macrophage responses to silk, *Biomaterials* 24 (2003) 3079–3085.
- [36] M. Santin, A. Motta, G. Freddi, M. Cannas, In vitro evaluation of the inflammatory potential of the silk fibroin, *J. Biomed. Mater. Res.* 46 (3) (1999) 382–389.
- [37] P.M. Cunniff, S.A. Fossey, M.A. Auerbach, J.W. Song, D.J. Kaplan, W.W. Adams, R.K. Eby, D. Mahoney, D.L. Vezie, Mechanical and thermal properties of the dragline silk from the spider *Nephila claviceps*, *Polym. Adv. Technol.* 5 (1994) 401–410.
- [38] M. Demura, T. Takekawa, T. Asakura, A. Nishikawa, Characterization of low-temperature-plasma treated silk fibroin fabrics by ESCA and the use of the fabrics as an enzyme-immobilization support, *Biomaterials* 13 (5) (1992) 276–280.
- [39] M. Tsukada, G. Freddi, N. Minoura, G. Allara, Preparation and application of porous silk fibroin materials, *J. Appl. Polym. Sci.* 54 (1994) 507–514.
- [40] J. Kikuchi, Y. Mitsui, T. Asakura, K. Hasuda, H. Araki, K. Owaku, Spectroscopic investigation of tertiary fold of staphylococcal protein A to explore its engineering application, *Biomaterials* 20 (7) (1999) 647–654.
- [41] T. Asakura, D.L. Kaplan, in: C.J. Arutzen (Ed.), *Encyclopedia of Agriculture Science*, vol. 4, Academic, New York, 1994, pp. 1–11.
- [42] Y. Mitsui, T. Asakura, H. Araki, K. Hasuda, Protein A with low molecular weight and its immobilization in silk membrane, *Rept. Prog. Polym. Phys. Jpn.* 32 (1989) 613–616.
- [43] M. Li, S. Lu, Z. Wu, H. Yan, J. Mo, L. Wang, Study on porous silk fibroin materials: I. Fine structure of freeze dried silk fibroin, *J. Appl. Polym. Sci.* 79 (12) (2001) 2185–2191.
- [44] B. Lotz, H.D. Keith, Crystal structure of poly(L-Ala-Gly)II. A model for silk. I. *J. Mol. Biol.* 61 (1) (1971) 201–215.
- [45] K.A. Granath, Solution properties of branched dextrans, *J. Colloid Sci.* 13 (1958) 308–328.
- [46] F.R. Senti, N.N. Hellman, N.H. Ludwig, G.E. Babcock, R. Tobin, C.A. Glass, B.L. Lamberts, Viscosity, sedimentation and light scattering properties of fractions of acid-hydrolysed dextran, *J. Polym. Sci.* 17 (1955) 527–546.
- [47] E. Bini, D.P. Knight, D.L. Kaplan, Mapping domain structures in silks from insects and spiders related to protein assembly, *J. Mol. Biol.* 335 (1) (2004) 27–40.
- [48] A. Lazaris, S. Arcidiacono, Y. Huang, J.F. Zhou, F. Duguay, N. Chretien, E.A. Welsh, J.W. Soares, C.N. Karatzas, Spider silk fibers spun from soluble recombinant silk produced in mammalian cells, *Science* 295 (5554) (2002) 472–476.
- [49] D. Kaplan, C. Mello, S. Fossey, S. Arcidiacono, S. Muller, in: K. McGrath, D. Kaplan (Eds.), *Protein-based Materials*, Birkhauser, Boston, 1998.
- [50] C.N. Pace, S. Trevino, E. Prabhakaran, J.M. Scholtz, Protein structure, stability and solubility in water and other solvents, *Philos. Trans. R. Soc. Lond., B Biol. Sci.* 359 (1448) (2004) 1225–1234 (discussion 1234–1225).
- [51] U.J. Kim, J. Park, H.J. Kim, M. Wada, D.L. Kaplan, Three-dimensional aqueous-derived biomaterial scaffolds from silk fibroin, *Biomaterials* 26 (15) (2005) 2775–2785.